

Variational inverse modelling within the Community Inversion Framework to assimilate $\delta^{13}\text{C}(\text{CH}_4)$ and CH_4 : a case study with model LMDz-SACS - Supplementary Material

Joël Thanwerdas^{1,*}, Marielle Saunois¹, Antoine Berchet¹, Isabelle Pison¹, Bruce H. Vaughn², Sylvia Englund Michel², and Philippe Bousquet¹

¹Laboratoire des Sciences du Climat et de l'Environnement, CEA-CNRS-UVSQ, IPSL, Gif-sur-Yvette, France.

²INSTAAR - University of Colorado, Boulder, CO, United States

Correspondence: J. Thanwerdas (joel.thanwerdas@lsce.ipsl.fr)

Supplementary material can be found here. References regarding the selected isotopic signature values are compiled in Text S1. Methods and references used to prescribe the CH_4 sinks are presented in Text S2. A demonstration of the Eq.(1) used to infer an isotopic signature for the soil uptake is provided in Text S3. Details regarding the stations that provided the assimilated data are given in Table S3 and Table S4. Emission and source signature values for each scenario are given in Table S5 and 5 Table S6, respectively. Finally, multiple additional figures mentioned in the main paper are also provided.

1 Text S1 : Source signature references

Data from literature have been compiled to assess region-specific or global values for source isotopic signatures associated to the multiple categories introduced in the main paper. These references are given here.

Rice cultivation Bréas et al. (2001) cited literature $\delta^{13}\text{C}(\text{CH}_4)_{\text{source}}$ values from rice paddies, ranging from -68 ‰ to -48 ‰. For this work, a value of -63 ‰ is used (Rice et al., 2016; Bousquet et al., 2006).

Waste Waste sector encompasses three different source categories : waste water (~ 49 %), solid waste (~ 49 %), agriculture waste burning and (~ 2 %). Values of -48 ‰ for waste water, -52 ‰ for solid waste and -23.6 ‰ for agriculture waste burning (Levin et al., 1993; Yamada et al., 2006; Townsend-Small et al., 2012; Bergamaschi et al., 1998; Chanton et al., 1999) is taken.

Biofuels-biomass burning Biofuels-biomass burning sector encompasses four very different emission sectors : biomass burning (~ 35 %), biofuel burning (~ 40 %), energy use (~ 20 %) and fossil fuel fires (~ 5 %). Regional values for biomass burning from -26.5 ‰ to -15.46 ‰ (Table S1), -20 ‰ for biofuel burning, -30 ‰ for energy use and -30 ‰ for fossil fuel fires are taken (Chanton et al., 2000).

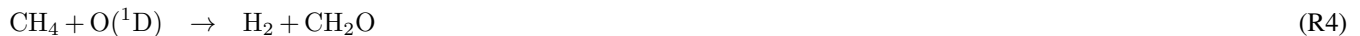
Oceanic fluxes Surface $\delta^{13}\text{C}(\text{CH}_4)_{\text{source}}$ values from various oceans in the world were found in a small range: roughly -44 ‰ to -40 ‰ (Brunskill et al., 2011; Holmes et al., 2000; Sansone et al., 2001). A value of -42 ‰ is used.

Termites A wide range of $\delta^{13}\text{C}(\text{CH}_4)_{\text{source}}$ signatures have been reported in the literature, from -93.8 ‰ to -54 ‰ (Bréas et al., 2001). For these simulations, $\delta^{13}\text{C}(\text{CH}_4)_{\text{source}}$ is taken to be -63 ‰.

Geological fluxes (onshore) A value of -50 ‰ is used (personal communication with Philippe Bousquet).

2 Text S2 : CH₄ sinks and associated KIEs in LMDz-SACS

CH₄ is removed in LMDz-SACS through the following chemical reactions with OH, O(¹D) and Cl:



We use the new chemistry parsing system introduced in the main paper to represent the chemical reactions with OH, O(¹D) and Cl. Fractionation values (KIE for Kinetic Isotope Effect) are prescribed to the different sinks. Here, KIE is defined by $\text{KIE} = k_{12}/k_{13}$ where k_{12} is the constant rate of the reaction involving ¹²CH₄ and k_{13} is the constant rate of the same reaction involving ¹³CH₄.

The three-dimensional and time-dependent oxidant concentration fields (OH, O(¹D) and Cl) were simulated by the LMDz General Circulation Model (GCM) coupled to the chemistry and aerosol model INCA [INteraction with Chemistry and Aerosols] (Folberth et al., 2006; Hauglustaine et al., 2004). Mean tropospheric Cl have been scaled to the values of Wang et al. (2019), i.e. 620 atoms cm⁻³.

15 Reaction constants in this paper are taken from Burkholder et al. (2015) and KIEs from Saueressig et al. (1995) for the reaction with Cl and from Saueressig et al. (2001) for reactions with OH and O(¹D). All reaction constants and associated values are reported in Table S2. Few studies have focused on assessing KIEs associated with CH₄ chemical sinks (especially for O(¹D) and Cl) within a wide temperature range and thus significant uncertainties still remain. We chose the KIE values for CH₄ + OH from Saueressig et al. (2001) as they indicate that this data is of considerably higher precision and experimental 20 reproducibility than earlier studies, in particular Cantrell et al. (1990).

The CH₄ atmospheric lifetime relative to chemical destruction is the ratio of the total CH₄ atmospheric burden to the atmospheric sink due to the chemical reactions with OH, O(¹D) and Cl. Our fields lead to an atmospheric chemical lifetime of 9.16 ± 0.12 years.

The soil uptake is accounted for as a negative source using the estimates taken from Ridgwell et al. (1999). Therefore we 25 define an effective $\delta^{13}\text{C(CH}_4)$ signature ($\delta^{13}\text{C(CH}_4)_{\text{source,eff}}$) based on the Kinetic Isotopic Effect (KIE_{soil}) of the soil uptake and $\delta^{13}\text{C(CH}_4)$ values at the surface :

$$\delta^{13}\text{C(CH}_4)_{\text{source,eff}} = \frac{1 + \delta^{13}\text{C(CH}_4)_{\text{atm}}}{\text{KIE}_{\text{soil}}} - 1 \quad (1)$$

$\delta^{13}\text{C(CH}_4)_{\text{atm}}$ denotes the atmospheric isotopic signal near the surface. A demonstration is given in Text S3. A KIE_{soil} of 1.020 (Snover and Quay, 2000; Reeburgh et al., 1997; Tyler et al., 1994; King et al., 1989) is chosen.

3 Text S3 : Demonstration of effective source signature for the soil uptake

Let L_{12} and L_{13} be the chemical losses of $^{12}\text{CH}_4$ and $^{13}\text{CH}_4$ through the soil uptake, respectively. k_{12} and k_{13} are the associated reaction constants. M_{12} , M_{13} and M_{air} are the molar masses of $^{12}\text{CH}_4$, $^{13}\text{CH}_4$ and dry air, respectively. $[^{12}\text{CH}_4]$ and $[^{13}\text{CH}_4]$ are the atmospheric concentrations of $^{12}\text{CH}_4$ and $^{13}\text{CH}_4$ at the surface. $\delta^{13}\text{C}(\text{CH}_4)_{\text{atm}}$ is the associated isotopic signal.

5 KIE_{soil} is defined such that :

$$\text{KIE}_{\text{soil}} = \frac{k_{12}}{k_{13}} \quad (2)$$

We also have, by definition :

$$L_{12} = k_{12} \cdot [^{12}\text{CH}_4] \quad (3)$$

$$L_{13} = k_{13} \cdot [^{13}\text{CH}_4] \quad (4)$$

$$10 \quad [^{13}\text{CH}_4] = (1 + \delta^{13}\text{C}(\text{CH}_4)_{\text{atm}}) \cdot R_{\text{std}} \cdot [^{12}\text{CH}_4] \quad (5)$$

We define $\delta^{13}\text{C}(\text{CH}_4)_{\text{source,eff}}$ the soil uptake effective isotopic signature :

$$\delta^{13}\text{C}(\text{CH}_4)_{\text{source,eff}} = \frac{\frac{L_{13}}{L_{12}}}{R_{\text{std}}} - 1 \quad (6)$$

By dividing (3) and (2) and using (4), we can get :

$$\frac{L_{13}}{L_{12}} = \frac{[^{13}\text{CH}_4]}{[^{12}\text{CH}_4]} \cdot \frac{1}{\text{KIE}_{\text{soil}}} \quad (7)$$

$$15 \quad \Rightarrow \delta^{13}\text{C}(\text{CH}_4)_{\text{source,eff}} = \frac{[^{13}\text{CH}_4]}{[^{12}\text{CH}_4]} \cdot \frac{1}{R_{\text{std}}} \cdot \frac{1}{\text{KIE}_{\text{soil}}} - 1 \quad (8)$$

$$\Rightarrow \delta^{13}\text{C}(\text{CH}_4)_{\text{source,eff}} = \frac{1 + \delta^{13}\text{C}(\text{CH}_4)_{\text{atm}}}{\text{KIE}_{\text{soil}}} - 1 \quad (9)$$

Defining $\alpha = \frac{1}{\text{KIE}_{\text{soil}}}$ and assuming that $\epsilon = \alpha - 1 \ll 1$, we find the formula of Snover and Quay (2000) :

$$\delta^{13}\text{C}(\text{CH}_4)_{\text{source,eff}} = \alpha \cdot \delta^{13}\text{C}(\text{CH}_4)_{\text{atm}} + (\alpha - 1) \quad (10)$$

$$\Rightarrow \delta^{13}\text{C}(\text{CH}_4)_{\text{source,eff}} \approx \delta^{13}\text{C}(\text{CH}_4)_{\text{atm}} + \epsilon \quad (11)$$

Table S1. Regional $\delta^{13}\text{C}(\text{CH}_4)_{\text{source}}$ isotopic signature values for biomass burning.

Region	Biomass burning
Global default	-26.5 ‰
Boreal North America	-26.5 ‰
Temperate North America	-26.5 ‰
Tropical South America	-18.15 ‰
Temperate South America	-19.53 ‰
Africa	-15.46 ‰
Europe	-26.5 ‰
Boreal Asia	-26.82 ‰
Temperate Asia	-19.16 ‰
Southeast Asia	-20.65 ‰
Australia	-26.5 ‰

Table S2. Reaction constants and KIEs of CH₄ chemical sinks. The reaction constants are taken from Burkholder et al. (2015).

Oxidant	KIE	Reference	Reaction constant (molecule ⁻¹ s ⁻¹)
OH	1.0039	Saueressig et al. (2001)	$2.45 \cdot 10^{-12} \cdot \exp(-1775/T)$
Cl	$1.043 \cdot \exp(6.455/T)$	Saueressig et al. (1995)	$7.1 \cdot 10^{-12} \cdot \exp(-1280/T)$
O(¹ D) - R3	1.013	Saueressig et al. (2001)	$1.125 \cdot 10^{-10}$
O(¹ D) - R4	1.013	Saueressig et al. (2001)	$3.75 \cdot 10^{-11}$

Table S3. List of CH₄ surface in-situ observation sites used in inversions.

Site code	Station name	Country/Territory	Network	Latitude	Longitude	Elevation (m a.s.l.)	Date range (MM/YYYY)
ALT	Alert	Canada	CSIRO	82.45° N	62.52° W	210	01/2012 - 12/2017
ALT	Alert	Canada	EC	82.45° N	62.52° W	210	01/2012 - 12/2016
ALT	Alert	Canada	NOAA	82.45° N	62.51° W	195	01/2012 - 12/2017
AMS	Amsterdam Island	France	LSCE	37.80° S	77.54° E	55	01/2012 - 12/2017
AMY	Anmyeon-do	Republic of Korea	KMA	36.53° N	126.32° E	47	01/2012 - 03/2017
ARH	Arrival Heights	New Zealand	NIWA	77.83° S	166.66° E	189	01/2012 - 01/2017
ASC	Ascension Island	United Kingdom	NOAA	7.97° S	14.40° W	90	01/2012 - 12/2017
ASK	Assekrem	Algeria	NOAA	23.26° N	5.63° E	2715	01/2012 - 12/2017
AZR	Terceira Island	Portugal	NOAA	38.75° N	27.08° W	24	01/2014 - 12/2017
BHD	Baring Head Station	New Zealand	NOAA	41.41° S	174.87° E	90	01/2012 - 12/2017
BKT	Bukit Kototabang	Indonesia	BMG-EMPA	0.20° S	100.32° E	864	01/2012 - 12/2013
BKT	Bukit Kototabang	Indonesia	NOAA	0.20° S	100.31° E	875	02/2013 - 04/2015
BMW	Tudor Hill	United Kingdom	NOAA	32.26° N	64.88° W	60	03/2012 - 12/2017
BRW	Barrow Atmospheric Baseline Observatory	United States	NOAA	71.32° N	156.60° W	11	01/2012 - 12/2016
CBA	Cold Bay	United States	NOAA	55.20° N	162.72° W	25	01/2012 - 12/2017
CFA	Cape Ferguson	Australia	CSIRO	19.28° S	147.05° E	2	01/2012 - 12/2017
CGO	Cape Grim	Australia	AGAGE	40.68° S	144.68° E	94	01/2012 - 03/2017
CGO	Cape Grim	Australia	CSIRO	40.68° S	144.68° E	94	01/2012 - 12/2017
CGO	Cape Grim	Australia	NOAA	40.68° S	144.69° E	164	01/2012 - 12/2017
CHR	Christmas Island	Republic of Kiribati	NOAA	1.70° N	157.15° W	5	01/2012 - 12/2017
CIB	Centro de Investigacion de la Baja Atmosfera (CIBA)	Spain	NOAA	41.81° N	4.93° W	850	01/2012 - 12/2017
CPT	Cape Point	South Africa	NOAA	34.35° S	18.49° E	260	01/2012 - 12/2017
CPT	Cape Point	South Africa	SAWS	34.35° S	18.48° E	230	01/2012 - 12/2016
CRZ	Crozet Island	France	NOAA	46.43° S	51.85° E	202	01/2012 - 09/2017
CYA	Casey Station	Australia	CSIRO	66.28° S	110.53° E	60	01/2012 - 12/2017
EIC	Easter Island	Chile	NOAA	27.15° S	109.45° W	55	01/2012 - 02/2014
ESP	Estevan Point	Canada	EC	49.38° N	126.55° W	39	01/2012 - 12/2016
GMI	Mariana Islands	Guam	NOAA	13.39° N	144.66° E	6	01/2012 - 06/2017

Table S3. List of surface in-situ observation sites used in inversions. *POC stations have been aggregated into a single line but all observations are used in the inversions.

Site code	Station name	Country/Territory	Network	Latitude	Longitude	Elevation (m a.s.l.)	Date range (MM/YYYY)
HBA	Halley Station	United Kingdom	NOAA	75.61° S	26.21° W	35	01/2012 - 01/2017
ICE	Storhofdi	Iceland	NOAA	63.40° N	20.29° W	127	01/2012 - 12/2017
IZO	Izana	Spain	AEMET	28.30° N	16.50° W	2367	01/2012 - 12/2016
IZO	Izana	Spain	NOAA	28.30° N	16.48° W	2377	01/2012 - 12/2017
JFJ	Jungfraujoch	Switzerland	EMPA	46.55° N	7.99° E	3580	01/2012 - 12/2016
KEY	Key Biscayne	United States	NOAA	25.67° N	80.20° W	6	01/2012 - 12/2017
KUM	Cape Kumukahi	United States	NOAA	19.52° N	154.82° W	3	01/2012 - 12/2017
LAU	Lauder	New Zealand	NIWA	45.03° S	169.67° E	370	01/2012 - 12/2016
LMP	Lampedusa	Italy	ENEA	35.52° N	12.63° E	45	01/2012 - 12/2014
LMP	Lampedusa	Italy	NOAA	35.52° N	12.62° E	50	01/2012 - 12/2017
LTO	Lamto	Ivory Coast	LSCE	6.22° N	5.03° W	155	01/2012 - 12/2017
MAA	Mawson	Australia	CSIRO	67.62° S	62.87° E	32	01/2012 - 12/2016
MEX	High Altitude Global Climate Observation Center	Mexico	NOAA	18.98° N	97.31° W	4469	01/2012 - 12/2017
MHD	Mace Head	Ireland	AGAGE	53.33° N	9.90° W	8	01/2012 - 03/2017
MHD	Mace Head	Ireland	LSCE	53.33° N	9.90° W	5	01/2012 - 12/2017
MHD	Mace Head	Ireland	NOAA	53.33° N	9.90° W	26	01/2012 - 12/2017
MID	Sand Island	United States	NOAA	28.22° N	177.37° W	8	01/2012 - 12/2017
MLO	Mauna Loa	United States	CSIRO	19.54° N	155.58° W	3397	01/2012 - 12/2016
MLO	Mauna Loa	United States	NOAA	19.53° N	155.58° W	3402	01/2012 - 12/2017
MQA	Macquarie Island	Australia	CSIRO	54.48° S	158.97° E	12	01/2012 - 12/2016
MWO	Mt. Wilson Observatory	United States	NOAA	34.22° N	118.06° W	1774	01/2012 - 12/2017
NAT	Farol De Mae Luiza Lighthouse	Brazil	NOAA	5.51° S	35.26° W	20	01/2012 - 12/2017
NMB	Gobabeb	Namibia	NOAA	23.58° S	15.03° E	461	05/2012 - 12/2017
NWR	Niwot Ridge	United States	NOAA	40.03° N	105.57° W	3526	10/2014 - 02/2015
PAL	Pallas-Sammaltunturi	Finland	FMI	67.97° N	24.12° E	560	01/2012 - 12/2016
PAL	Pallas-Sammaltunturi	Finland	NOAA	67.96° N	24.11° E	570	01/2012 - 11/2014
POC*	Pacific Ocean	N/A	NOAA	35° S - 30° N	178°W - 178° E	20	01/2012 - 07/2017
PON	Pondichery	India	LSCE	12.01° N	79.86° E	30	01/2012 - 03/2015
PSA	Palmer Station	United States	NOAA	64.92° S	64.00° W	15	01/2012 - 12/2017
RPB	Ragged Point	Barbados	AGAGE	13.17° N	59.43° W	45	01/2012 - 02/2017
RPB	Ragged Point	Barbados	NOAA	13.16° N	59.43° W	20	01/2012 - 12/2017

Table S3. List of surface in-situ observation sites used in inversions. *WPC stations have been aggregated into a single line but all observations are used in the inversions.

Site code	Station name	Country/Territory	Network	Latitude	Longitude	Elevation (m a.s.l.)	Date range (MM/YYYY)
SEY	Mahe Island	Seychelles	NOAA	4.68° S	55.53° E	7	01/2012 - 12/2017
SHM	Shemya Island	United States	NOAA	52.72° N	174.10° E	28	01/2012 - 11/2017
SMO	Tutuila	American Samoa	AGAGE	14.24° S	170.57° W	42	01/2012 - 03/2017
SMO	Tutuila	American Samoa	NOAA	14.25° S	170.57° W	47	01/2012 - 12/2017
SPO	South Pole	United States	CSIRO	89.98° S	24.80° W	2810	01/2012 - 11/2016
SPO	South Pole	United States	NOAA	89.98° S	24.80° W	2815	01/2012 - 12/2017
STR	Sutro Tower	United States	NOAA	37.76° N	122.45° W	486	01/2012 - 12/2017
SUM	Summit	Greenland	NOAA	72.60° N	38.42° W	3214	01/2012 - 07/2017
SYO	Syowa Station	Japan	NOAA	69.00° S	39.58° E	16	01/2012 - 01/2017
TDF	Tierra Del Fuego	Argentina	NOAA	54.87° S	68.48° W	20	01/2012 - 12/2013
TER	Teriberka	Russian Federation	MGO	69.20° N	35.10° E	40	01/2012 - 12/2016
THD	Trinidad Head	United States	AGAGE	41.05° N	124.15° W	120	01/2012 - 03/2017
THD	Trinidad Head	United States	NOAA	41.03° N	124.15° W	112	01/2012 - 12/2015
TIK	Hydrometeorological Observatory of Tiksi	Russia	MGO	71.59° N	128.92° E	8	01/2012 - 03/2016
TIK	Hydrometeorological Observatory of Tiksi	Russia	NOAA	71.59° N	128.92° E	8	02/2012 - 12/2016
TR3	Traïnou	France	LSCE	47.96° N	2.11° E	131	01/2012 - 12/2017
USH	Ushuaia	Argentina	NOAA	54.85° S	68.31° W	32	01/2012 - 12/2017
UTA	Wendover	United States	NOAA	39.90° N	113.72° W	1332	01/2012 - 12/2017
UUM	Ulaan Uul	Mongolia	NOAA	44.45° N	111.10° E	1012	01/2012 - 12/2017
WIS	Weizmann Institute of Science at the Arava Institute	Israel	NOAA	30.86° N	34.78° E	482	01/2012 - 12/2017
WKT	Moody	United States	NOAA	31.32° N	97.33° W	256	01/2012 - 02/2015
WLG	Mt. Waliguan	Peoples Republic of China	CMANOAA	36.27° N	100.92° E	3815	01/2012 - 10/2017
WPC*	Western Pacific Cruise	N/A	NOAA	30° S 30° N	137° E - 170° E	10	06/2012 - 06/2013
ZEP	Ny-Alesund	Norway and Sweden	NOAA	78.91° N	11.89° E	479	01/2012 - 12/2017

Table S4. List of $\delta^{13}\text{C}(\text{CH}_4)$ surface in-situ observation sites used in inversions.

Site code	Station name	Country/Territory	Network	Latitude	Longitude	Elevation (m a.s.l.)	Date range (MM/YYYY)
ALT	Alert	Canada	NOAA/INSTAAR	82.45° N	62.51° W	195	01/2012 - 12/2017
AMY	Anmyeon-do	Republic of Korea	NOAA/INSTAAR	36.54° N	126.33° E	125	12/2013 - 12/2017
ASC	Ascension Island	United Kingdom	NOAA/INSTAAR	7.97° S	14.40° W	90	01/2012 - 12/2017
AZR	Terceira Island	Portugal	NOAA/INSTAAR	38.77° N	27.38° W	24	06/2012 - 12/2017
BHD	Baring Head Station	New Zealand	NOAA/INSTAAR	41.41° S	174.87° E	90	01/2012 - 12/2014
BRW	Barrow Atmospheric Baseline Observatory	United States	NOAA/INSTAAR	71.32° N	156.61° W	16	01/2012 - 12/2017
CBA	Cold Bay	United States	NOAA/INSTAAR	55.21° N	162.72° W	57	01/2012 - 12/2017
CGO	Cape Grim	Australia	NOAA/INSTAAR	40.68° S	144.69° E	164	01/2012 - 12/2017
KUM	Cape Kumukahi	United States	NOAA/INSTAAR	19.52° N	154.82° W	8	01/2012 - 12/2017
MEX	High Altitude Global Climate Observation Center	Mexico	NOAA/INSTAAR	18.98° N	97.31° W	4469	01/2012 - 12/2017
MHD	Mace Head	Ireland	NOAA/INSTAAR	53.33° N	9.90° W	26	01/2012 - 12/2017
MLO	Mauna Loa	United States	NOAA/INSTAAR	19.54° N	155.58° W	3402	01/2012 - 12/2017
NWR	Niwot Ridge	United States	NOAA/INSTAAR	40.05° N	105.58° W	3526	01/2012 - 06/2012
SMO	Tutuila	American Samoa	NOAA/INSTAAR	14.25° S	170.56° W	47	01/2012 - 12/2017
SPO	South Pole	United States	NOAA/INSTAAR	89.98° S	24.80° W	2815	01/2012 - 12/2017
SUM	Summit	Greenland	NOAA/INSTAAR	72.60° N	38.42° W	3214	01/2012 - 12/2017
WLG	Mt. Waliguan	Peoples Republic of China	NOAA/INSTAAR	36.29° N	100.90° E	3815	01/2012 - 12/2017
ZEP	Ny-Alesund	Norway and Sweden	NOAA/INSTAAR	78.91° N	11.89° E	479	01/2012 - 12/2017

Table S5. Global and regional methane emissions by source category and region (Tg yr^{-1}) for all configurations. Values are averages over the 2014-2015 period.

Others										
	PRIOR REF	NOISO	REF	S1	S2	S3	T1	T2	T3	T4
Biofuels-Biomass	1	1	1	1	1	1	1	1	1	1
Microbial	4	4	4	4	4	4	4	4	4	4
Fossil Fuels	5	5	5	5	5	5	5	5	5	5
Natural	8	8	8	8	8	8	8	8	8	8
Wetlands	2	2	2	2	2	2	2	2	2	2
Total	19	19	19	19	19	19	19	19	19	19
U.S										
	PRIOR REF	NOISO	REF	S1	S2	S3	T1	T2	T3	T4
Biofuels-Biomass	1	1	1	1	1	1	1	1	1	1
Microbial	21	22	22	22	22	22	22	22	22	21
Fossil Fuels	13	13	14	14	14	14	14	14	14	15
Natural	2	2	2	2	2	2	2	2	2	2
Wetlands	17	17	17	17	17	17	17	17	16	16
Total	55	55	56	56	56	56	56	56	56	56
Canada										
	PRIOR REF	NOISO	REF	S1	S2	S3	T1	T2	T3	T4
Biofuels-Biomass	2	1	2	2	2	2	2	2	3	3
Microbial	2	2	2	2	2	2	2	2	2	2
Fossil Fuels	2	2	2	2	2	2	2	2	2	2
Natural	1	1	1	1	1	1	1	1	1	1
Wetlands	27	23	21	21	21	21	22	23	16	18
Total	34	30	29	29	29	29	30	30	24	26
South America										
	PRIOR REF	NOISO	REF	S1	S2	S3	T1	T2	T3	T4
Biofuels-Biomass	2	2	2	2	2	2	2	2	2	3
Microbial	29	31	30	30	30	31	30	30	29	30
Fossil Fuels	5	6	6	6	6	6	6	6	6	6
Natural	5	5	5	5	5	5	5	5	5	5
Wetlands	49	55	53	53	53	54	53	52	51	50
Total	91	99	96	96	97	97	96	96	93	93
Africa										
	PRIOR REF	NOISO	REF	S1	S2	S3	T1	T2	T3	T4
Biofuels-Biomass	8	8	9	9	9	9	9	9	9	10
Microbial	25	26	25	25	25	25	25	25	25	25
Fossil Fuels	13	13	14	14	14	14	14	14	14	15
Natural	4	4	4	4	4	4	4	4	4	4
Wetlands	26	28	28	28	28	28	28	27	27	26
Total	77	80	80	80	80	80	80	80	80	80

Table S5. Global and regional methane emissions by source category and region (Tg yr^{-1}) for all configurations. Values are averages over the 2014-2015 period.

Europe										
	PRIOR REF	NOISO	REF	S1	S2	S3	T1	T2	T3	T4
Biofuels-Biomass	1	1	1	1	1	1	1	1	1	1
Microbial	21	20	20	20	20	20	20	20	20	19
Fossil Fuels	6	6	6	6	6	6	6	6	7	7
Natural	2	2	2	2	2	2	2	2	2	2
Wetlands	4	4	4	4	4	4	4	4	4	4
Total	34	33	34	34	34	34	34	33	34	33
Russia										
	PRIOR REF	NOISO	REF	S1	S2	S3	T1	T2	T3	T4
Biofuels-Biomass	2	2	2	2	2	2	2	2	2	2
Microbial	5	5	5	5	5	5	5	5	5	5
Fossil Fuels	12	12	12	12	12	12	12	12	13	13
Natural	3	3	3	3	3	3	3	3	3	3
Wetlands	13	12	12	12	13	13	13	13	11	12
Total	35	34	35	35	35	35	36	35	35	35
Temperate Asia										
	PRIOR REF	NOISO	REF	S1	S2	S3	T1	T2	T3	T4
Biofuels-Biomass	3	3	3	3	3	3	3	3	3	3
Microbial	55	56	54	54	55	54	54	54	51	51
Fossil Fuels	26	27	28	28	28	28	29	29	30	31
Natural	7	7	7	7	7	7	7	7	7	7
Wetlands	12	13	13	13	13	13	13	12	12	11
Total	103	105	105	106	106	105	105	105	104	104
China										
	PRIOR REF	NOISO	REF	S1	S2	S3	T1	T2	T3	T4
Biofuels-Biomass	5	5	5	5	5	5	5	5	5	5
Microbial	36	32	29	28	29	29	31	29	26	26
Fossil Fuels	25	19	24	24	23	23	21	22	33	29
Natural	1	1	1	1	1	1	1	1	1	1
Wetlands	5	5	5	5	5	5	5	5	5	5
Total	72	61	64	63	63	63	63	62	70	66
South East Asia										
	PRIOR REF	NOISO	REF	S1	S2	S3	T1	T2	T3	T4
Biofuels-Biomass	8	9	11	10	10	10	10	11	15	18
Microbial	22	23	23	23	23	23	22	23	22	22
Fossil Fuels	7	7	8	8	8	8	8	8	8	8
Natural	3	4	4	4	4	4	3	4	4	4
Wetlands	22	23	22	22	22	22	22	22	22	21
Total	63	66	66	66	67	66	66	67	70	72

Table S5. Global and regional methane emissions by source category and region (Tg yr^{-1}) for all configurations. Values are averages over the 2014-2015 period.

Oceania										
	PRIOR REF	NOISO	REF	S1	S2	S3	T1	T2	T3	T4
Biofuels-Biomass	0	0	1	1	1	1	1	1	1	1
Microbial	5	5	4	4	4	4	4	4	4	4
Fossil Fuels	2	2	2	2	2	2	2	2	2	2
Natural	1	1	1	1	1	1	1	1	1	1
Wetlands	3	3	3	3	3	3	3	3	3	3
Total	11	11	11	11	11	11	11	11	11	11
Global										
	PRIOR REF	NOISO	REF	S1	S2	S3	T1	T2	T3	T4
Biofuels-Biomass	33	33	37	37	37	36	37	38	44	47
Microbial	226	226	220	219	221	220	220	220	211	210
Fossil Fuels	116	111	119	120	120	119	118	119	134	132
Natural	38	38	38	39	39	38	39	39	39	39
Wetlands	180	185	180	179	181	181	182	180	169	167
Total	593	594	594	594	597	594	595	594	596	595

Table S6. Global and regional source signatures by source category and region (Tg yr^{-1}) for all configurations. Values are flux-weighted with posterior fluxes and averaged over the 2014–2015 period.

Others									
	PRIOR REF	REF	S1	S2	S3	T1	T2	T3	T4
Biofuels-Biomass	-24.8	-24.4	-24.4	-24.4	-24.5	-24.4	-22.3	-24.8	-22.6
Microbial	-57.2	-56.9	-56.8	-56.8	-56.9	-57.0	-58.7	-57.1	-59.1
Fossil Fuels	-45.1	-44.9	-44.9	-44.9	-44.9	-44.9	-43.2	-45.1	-43.4
Natural	-42.7	-42.7	-42.7	-42.7	-42.7	-42.6	-49.9	-42.7	-49.9
Wetlands	-60.1	-59.9	-59.9	-59.9	-59.9	-59.9	-60.0	-60.1	-60.2
Total	-47.3	-47.1	-47.0	-47.0	-47.1	-47.0	-49.8	-47.0	-49.7
U.S									
	PRIOR REF	REF	S1	S2	S3	T1	T2	T3	T4
Biofuels-Biomass	-24.8	-24.7	-24.7	-24.7	-24.7	-24.7	-22.7	-24.8	-22.7
Microbial	-59.0	-58.5	-58.4	-58.4	-58.4	-58.5	-58.5	-58.9	-59.1
Fossil Fuels	-45.3	-44.8	-44.7	-44.7	-44.7	-44.7	-43.0	-45.2	-43.4
Natural	-49.7	-49.6	-49.6	-49.6	-49.7	-49.6	-49.9	-49.6	-49.9
Wetlands	-61.7	-60.6	-60.4	-60.5	-60.7	-60.3	-60.3	-61.3	-61.0
Total	-55.6	-54.8	-54.6	-54.7	-54.8	-54.7	-54.2	-55.0	-54.4
Canada									
	PRIOR REF	REF	S1	S2	S3	T1	T2	T3	T4
Biofuels-Biomass	-24.8	-24.0	-24.0	-24.0	-24.3	-24.0	-22.5	-24.8	-23.0
Microbial	-57.2	-56.8	-56.7	-56.8	-56.8	-56.8	-58.6	-57.1	-59.1
Fossil Fuels	-54.7	-54.2	-54.1	-54.1	-54.1	-54.1	-43.0	-54.7	-43.4
Natural	-44.8	-44.8	-44.8	-44.8	-44.8	-44.8	-49.9	-44.8	-49.9
Wetlands	-70.0	-66.8	-66.2	-66.5	-67.1	-65.8	-59.7	-69.4	-62.1
Total	-65.2	-61.3	-60.6	-61.0	-61.6	-60.4	-55.6	-60.6	-55.8
South America									
	PRIOR REF	REF	S1	S2	S3	T1	T2	T3	T4
Biofuels-Biomass	-22.0	-21.8	-21.8	-21.8	-21.9	-21.8	-22.5	-22.0	-22.6
Microbial	-58.8	-58.3	-58.2	-58.3	-58.3	-58.3	-58.4	-58.8	-59.1
Fossil Fuels	-46.5	-46.3	-46.3	-46.3	-46.3	-46.3	-43.3	-46.5	-43.4
Natural	-57.2	-57.2	-57.2	-57.2	-57.2	-57.2	-49.9	-57.2	-49.9
Wetlands	-57.8	-56.6	-56.4	-56.5	-56.6	-56.2	-58.2	-57.7	-59.7
Total	-56.6	-55.7	-55.6	-55.7	-55.8	-55.5	-56.1	-56.4	-57.0
Africa									
	PRIOR REF	REF	S1	S2	S3	T1	T2	T3	T4
Biofuels-Biomass	-21.0	-20.9	-20.9	-20.9	-20.9	-20.9	-22.4	-21.0	-22.6
Microbial	-59.7	-59.4	-59.3	-59.3	-59.4	-59.4	-58.7	-59.7	-59.1
Fossil Fuels	-44.0	-43.7	-43.6	-43.6	-43.7	-43.6	-43.1	-43.9	-43.4
Natural	-55.7	-55.7	-55.6	-55.6	-55.7	-55.6	-49.9	-55.7	-49.9
Wetlands	-55.4	-54.7	-54.6	-54.6	-54.7	-54.5	-59.0	-55.3	-59.9
Total	-51.2	-50.6	-50.6	-50.6	-50.7	-50.5	-51.5	-50.6	-51.6

Table S6. Global and regional source signatures by source category and region (Tg yr^{-1}) for all configurations. Values are averages over the 2014-2015 period.

Europe									
	PRIOR REF	REF	S1	S2	S3	T1	T2	T3	T4
Biofuels-Biomass	-24.4	-24.3	-24.3	-24.3	-24.3	-24.3	-22.6	-24.4	-22.6
Microbial	-58.7	-57.9	-57.8	-57.9	-58.0	-57.9	-58.3	-58.7	-59.1
Fossil Fuels	-44.4	-44.1	-44.1	-44.1	-44.1	-44.2	-43.1	-44.4	-43.4
Natural	-47.5	-47.4	-47.4	-47.4	-47.4	-47.4	-49.9	-47.5	-49.9
Wetlands	-66.7	-66.4	-66.4	-66.4	-66.4	-66.3	-61.0	-66.6	-61.2
Total	-55.4	-54.7	-54.7	-54.7	-54.8	-54.8	-54.2	-55.1	-54.5
Russia									
	PRIOR REF	REF	S1	S2	S3	T1	T2	T3	T4
Biofuels-Biomass	-24.8	-24.5	-24.5	-24.5	-24.6	-24.5	-22.7	-24.8	-22.9
Microbial	-56.0	-55.6	-55.6	-55.6	-55.7	-55.6	-58.7	-55.9	-59.1
Fossil Fuels	-44.3	-43.9	-43.8	-43.9	-44.0	-43.9	-43.0	-44.3	-43.4
Natural	-47.8	-47.8	-47.7	-47.7	-47.8	-47.7	-49.9	-47.8	-49.9
Wetlands	-68.7	-67.2	-67.0	-67.2	-67.5	-66.9	-61.3	-68.4	-62.3
Total	-54.5	-53.2	-53.1	-53.3	-53.6	-53.2	-51.4	-53.0	-51.3
Temperate Asia									
	PRIOR REF	REF	S1	S2	S3	T1	T2	T3	T4
Biofuels-Biomass	-22.5	-22.4	-22.4	-22.4	-22.4	-22.4	-22.5	-22.4	-22.6
Microbial	-59.2	-57.7	-57.5	-57.6	-57.6	-58.2	-57.3	-59.2	-59.1
Fossil Fuels	-44.0	-43.4	-43.4	-43.4	-43.4	-43.3	-42.7	-44.1	-43.4
Natural	-50.0	-49.7	-49.7	-49.7	-49.8	-49.7	-49.7	-50.0	-49.9
Wetlands	-58.5	-57.4	-57.2	-57.3	-57.5	-57.1	-60.2	-58.5	-61.4
Total	-53.6	-52.3	-52.1	-52.2	-52.3	-52.4	-52.1	-52.9	-52.8
China									
	PRIOR REF	REF	S1	S2	S3	T1	T2	T3	T4
Biofuels-Biomass	-22.3	-22.2	-22.1	-22.2	-22.2	-22.1	-22.4	-22.3	-22.6
Microbial	-58.8	-57.2	-57.0	-57.1	-57.3	-58.1	-57.0	-58.9	-59.1
Fossil Fuels	-37.7	-36.5	-36.4	-36.4	-36.7	-36.6	-41.5	-37.4	-43.4
Natural	-49.0	-49.0	-49.0	-49.0	-49.0	-49.0	-49.9	-49.0	-49.9
Wetlands	-58.5	-58.1	-58.0	-58.1	-58.1	-58.0	-60.6	-58.5	-61.2
Total	-48.9	-46.8	-46.5	-46.7	-47.0	-48.0	-48.9	-45.8	-49.2
South East Asia									
	PRIOR REF	REF	S1	S2	S3	T1	T2	T3	T4
Biofuels-Biomass	-23.1	-21.7	-21.9	-21.6	-22.2	-21.7	-21.2	-22.9	-22.7
Microbial	-59.8	-58.8	-58.7	-58.8	-58.8	-59.4	-57.9	-59.8	-59.1
Fossil Fuels	-46.0	-45.7	-45.7	-45.7	-45.7	-45.7	-43.1	-46.0	-43.4
Natural	-54.2	-54.1	-54.1	-54.1	-54.1	-54.1	-49.9	-54.1	-49.9
Wetlands	-58.5	-57.9	-57.9	-57.9	-58.0	-57.8	-59.3	-58.5	-60.0
Total	-52.6	-50.9	-50.9	-50.9	-51.2	-51.1	-50.1	-49.7	-48.5

Table S6. Global and regional source signatures by source category and region (Tg yr^{-1}) for all configurations. Values are averages over the 2014-2015 period.

Oceania									
	PRIOR REF	REF	S1	S2	S3	T1	T2	T3	T4
Biofuels-Biomass	-24.8	-24.7	-24.7	-24.7	-24.7	-24.7	-22.6	-24.8	-22.6
Microbial	-62.8	-62.7	-62.7	-62.7	-62.7	-62.6	-58.9	-62.9	-59.1
Fossil Fuels	-50.7	-50.6	-50.6	-50.6	-50.6	-50.6	-43.3	-50.7	-43.4
Natural	-49.1	-49.1	-49.1	-49.1	-49.1	-49.1	-49.9	-49.1	-49.9
Wetlands	-56.5	-56.4	-56.3	-56.4	-56.4	-56.3	-59.2	-56.5	-59.4
Total	-56.0	-55.8	-55.7	-55.7	-55.8	-55.7	-53.9	-55.8	-54.0
Global									
	PRIOR REF	REF	S1	S2	S3	T1	T2	T3	T4
Biofuels-Biomass	-22.6	-22.1	-22.2	-22.1	-22.3	-22.1	-22.0	-22.7	-22.7
Microbial	-59.1	-58.2	-58.0	-58.1	-58.2	-58.4	-58.0	-59.1	-59.1
Fossil Fuels	-43.4	-42.9	-42.9	-42.9	-43.1	-43.1	-42.7	-43.1	-43.4
Natural	-50.0	-49.9	-49.9	-49.9	-49.9	-49.8	-49.9	-49.9	-49.9
Wetlands	-60.8	-59.1	-58.9	-59.0	-59.2	-58.8	-59.4	-59.9	-60.6
Total	-53.9	-52.6	-52.5	-52.6	-52.8	-52.7	-52.5	-52.4	-52.6

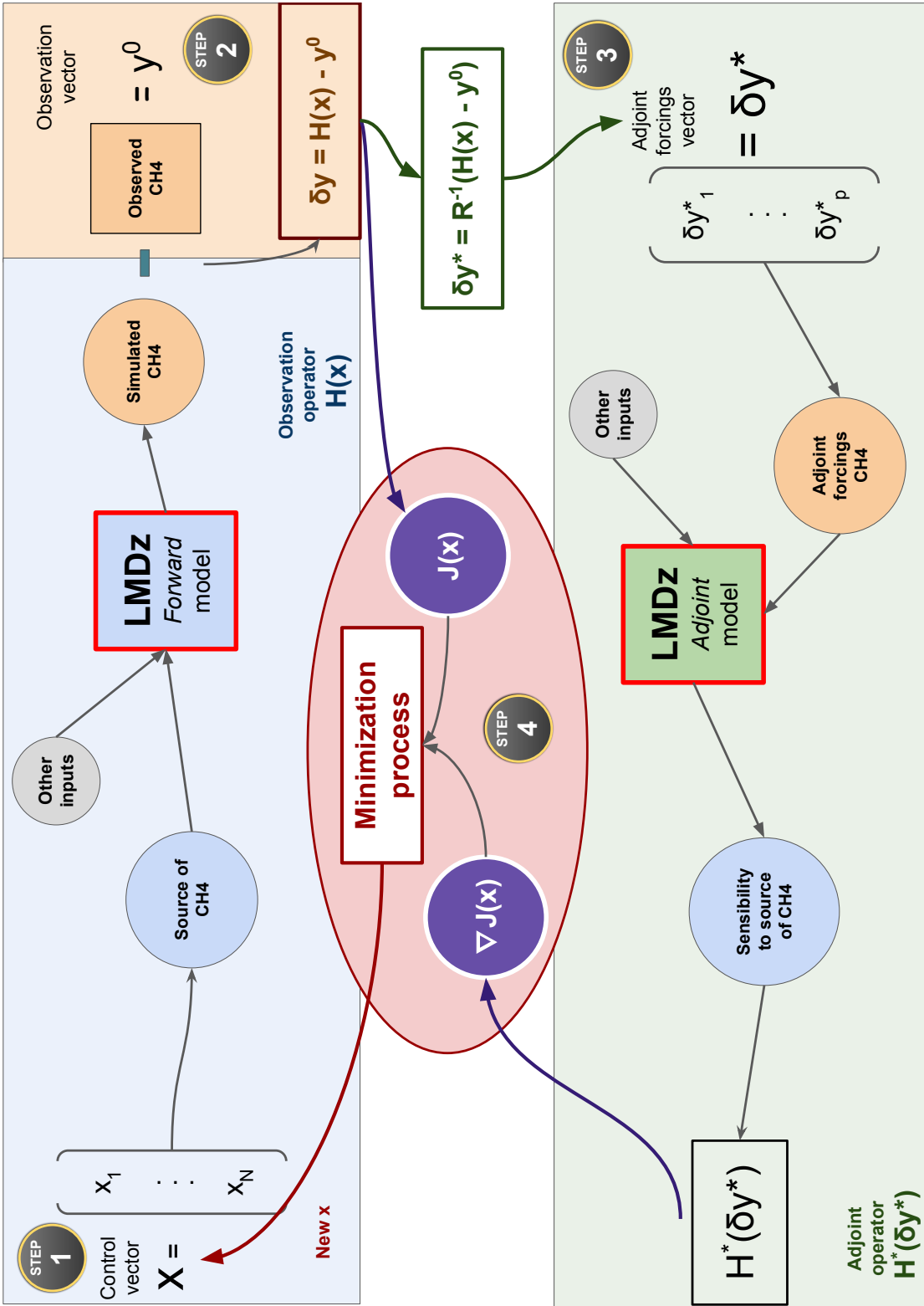


Figure S1. The minimization iteration process used in the previous system. The "step" black circles with gold border indicates the reading direction to follow. Step 1 (blue rectangle) refers to a forward run. Step 2 (orange rectangle) refers to the forward and adjoint operations required to compare observations and simulated values. Step 3 (green rectangle) refers to an adjoint run. This step must be read from the right to the left. Step 4 (red ellipse) refers to the minimization of the cost function operated by the dedicated minimization algorithm. Note that results of Step 2 are used both in the minimization process (red ellipse) and as inputs for Step 3.

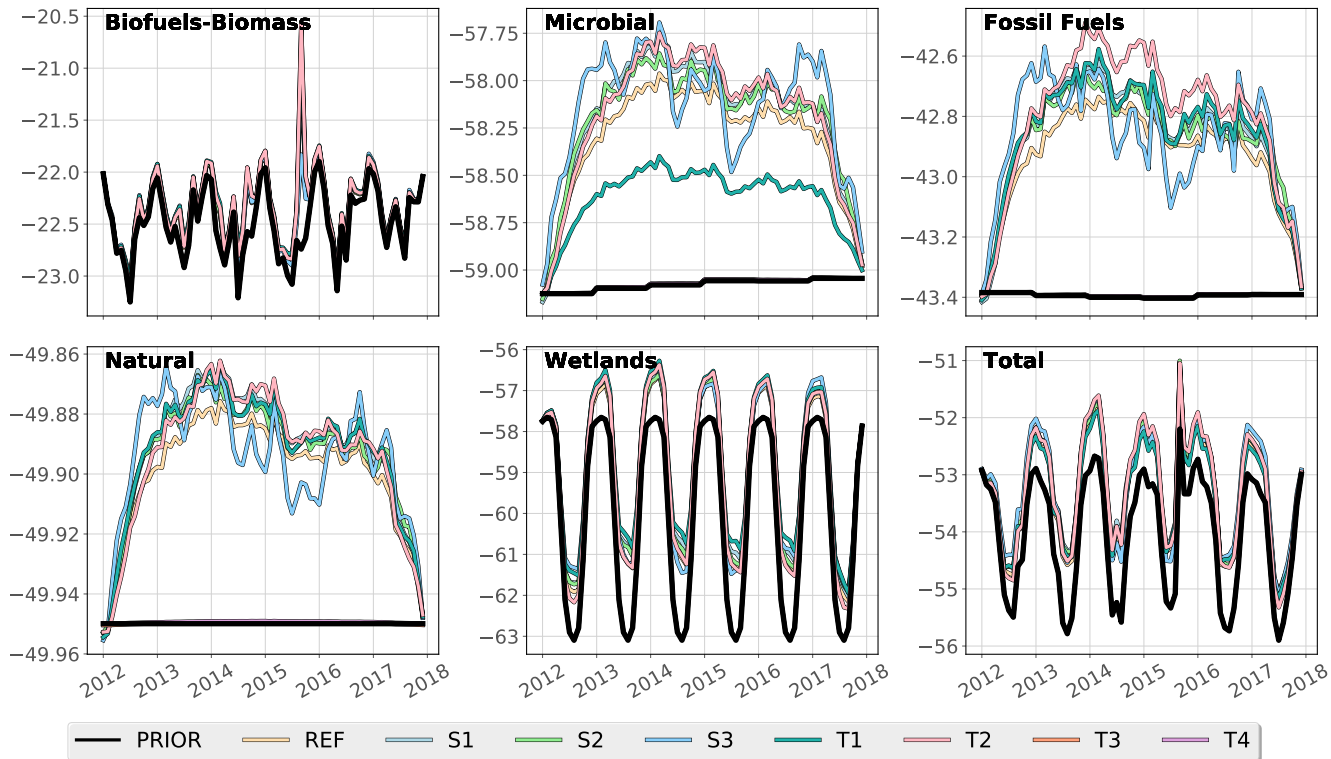


Figure S2. Time-series of source signatures for each category inferred with REF. Source signatures are flux-weighted averaged using prior fluxes.

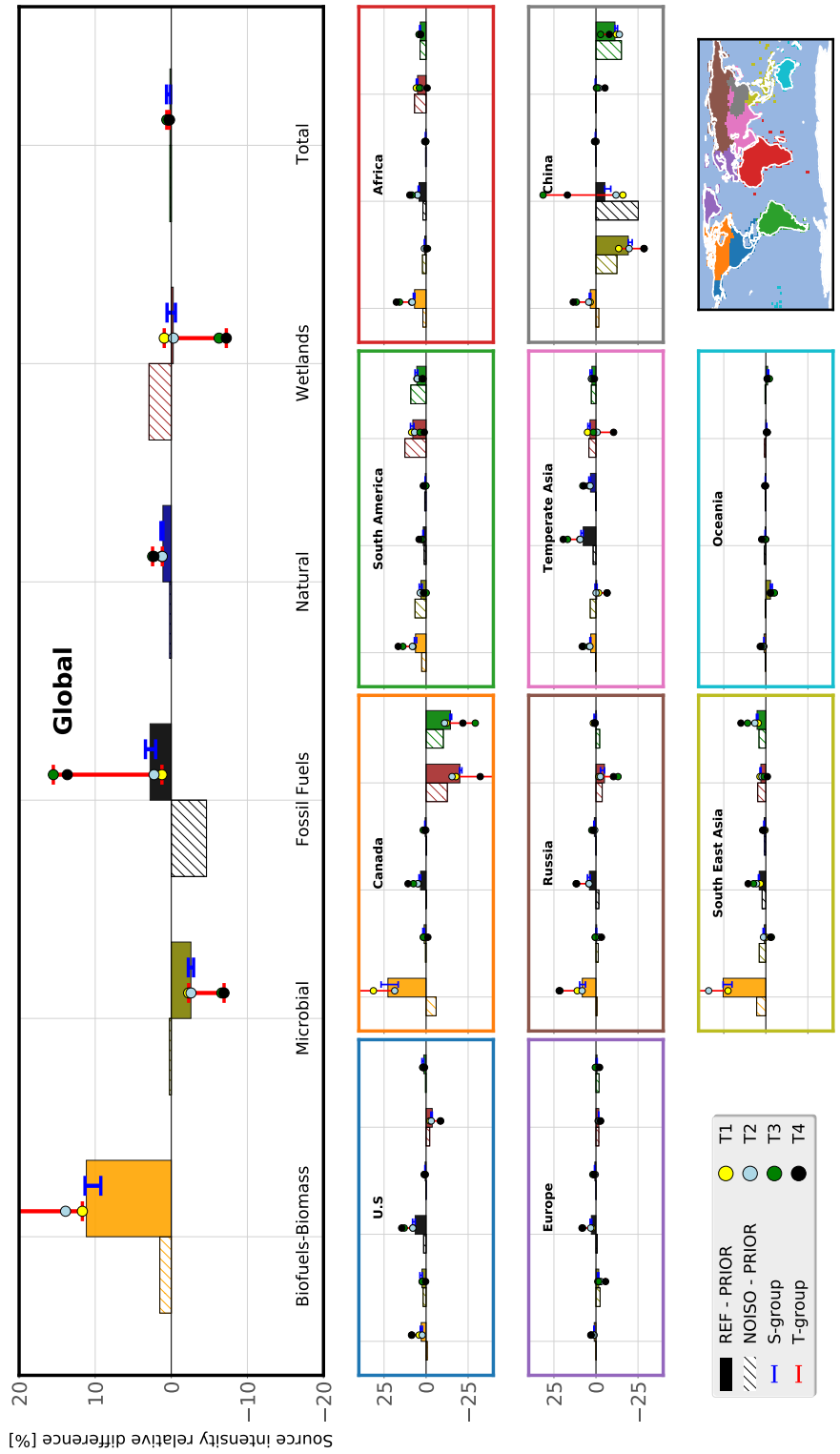


Figure S3. Same as Figure 6 from the main paper but with relative values (in %).

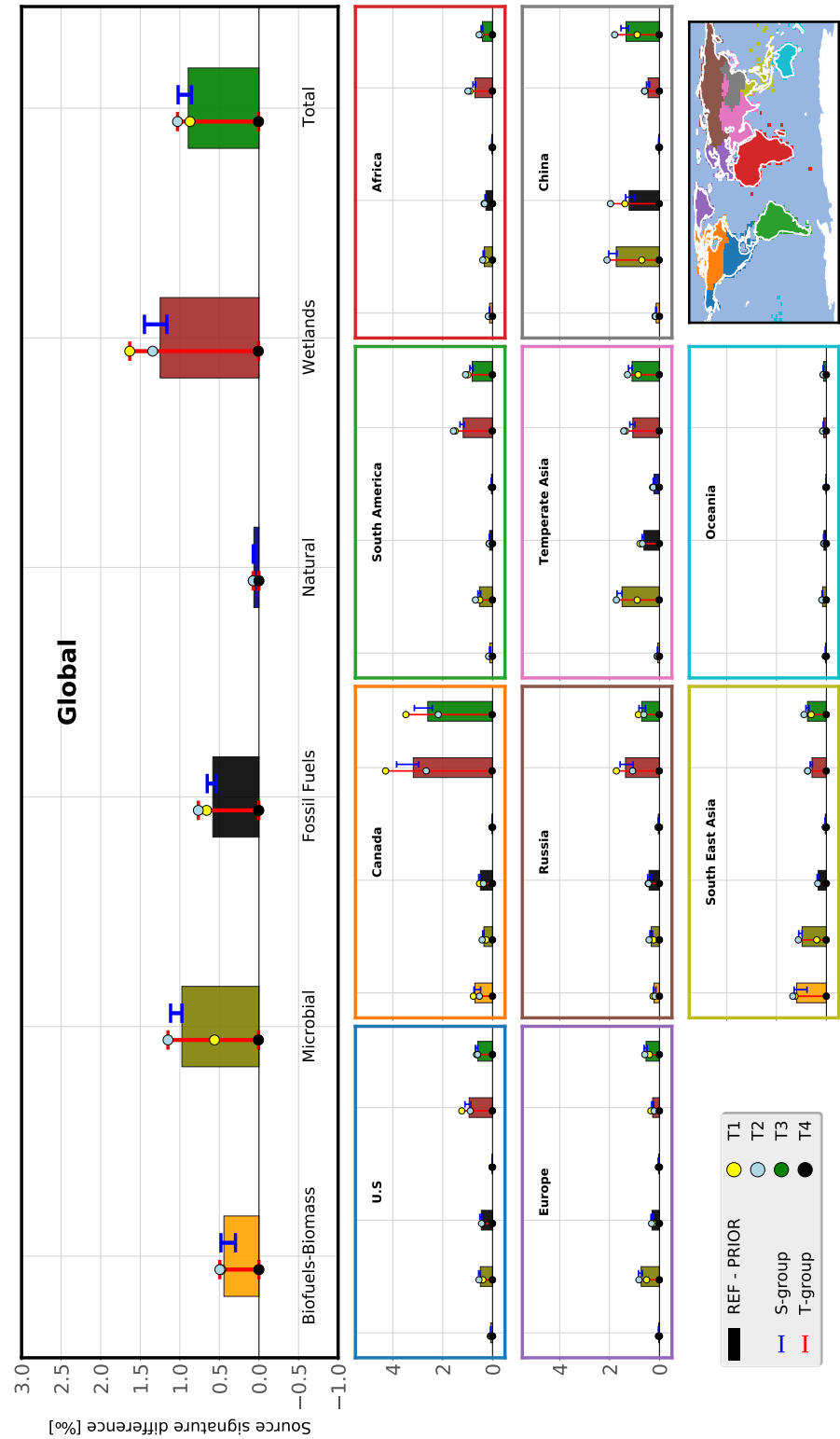


Figure S4. Same as Figure 7 from the main paper but prior fluxes are used to compute flux-weighted averages.

References

- Bergamaschi, P., Lubina, C., Königstedt, R., Fischer, H., Veltkamp, A. C., and Zwaagstra, O.: Stable isotopic signatures ($\delta^{13}\text{C}$, δD) of methane from European landfill sites, *Journal of Geophysical Research: Atmospheres*, 103, 8251–8265, <https://doi.org/10.1029/98JD00105>, <https://agupubs.onlinelibrary.wiley.com/doi/abs/10.1029/98JD00105>, 1998.
- 5 Bousquet, P., Ciais, P., Miller, J. B., Dlugokencky, E. J., Hauglustaine, D. A., Prigent, C., Van der Werf, G. R., Peylin, P., Brunke, E.-G., Carouge, C., Langenfelds, R. L., Lathière, J., Papa, F., Ramonet, M., Schmidt, M., Steele, L. P., Tyler, S. C., and White, J.: Contribution of anthropogenic and natural sources to atmospheric methane variability, *Nature*, 443, 439–443, <https://doi.org/10.1038/nature05132>, <http://www.nature.com/articles/nature05132>, 2006.
- 10 Brunskill, G. J., Burns, K. A., and Zagorskis, I.: Natural flux of greenhouse methane from the Timor Sea to the atmosphere, *Journal of Geophysical Research: Biogeosciences*, 116, <https://doi.org/10.1029/2010JG001444>, <http://agupubs.onlinelibrary.wiley.com/doi/abs/10.1029/2010JG001444>, 2011.
- Bréas, O., Guillou, C., Reniero, F., and Wada, E.: The Global Methane Cycle: Isotopes and Mixing Ratios, Sources and Sinks, *Isotopes in Environmental and Health Studies*, 37, 257–379, <https://doi.org/10.1080/10256010108033302>, <https://doi.org/10.1080/10256010108033302>, 2001.
- 15 Burkholder, J. B., Abbatt, J. P. D., Huie, R. E., Kurylo, M. J., Wilmouth, D. M., Sander, S. P., Barker, J. R., Kolb, C. E., Orkin, V. L., and Wine, P. H.: *JPL Publication 15-10: Chemical Kinetics and Photochemical Data for Use in Atmospheric Studies*, p. 1392, 2015.
- Cantrell, C. A., Shetter, R. E., McDaniel, A. H., Calvert, J. G., Davidson, J. A., Lowe, D. C., Tyler, S. C., Cicerone, R. J., and Greenberg, J. P.: Carbon kinetic isotope effect in the oxidation of methane by the hydroxyl radical, *Journal of Geophysical Research: Atmospheres*, 95, 22 455–22 462, [https://doi.org/https://doi.org/10.1029/JD095iD13p22455](https://doi.org/10.1029/JD095iD13p22455), <http://agupubs.onlinelibrary.wiley.com/doi/abs/10.1029/JD095iD13p22455>, 1990.
- 20 Chanton, J. P., Rutkowski, C. M., and Mosher, B.: Quantifying Methane Oxidation from Landfills Using Stable Isotope Analysis of Downwind Plumes, *Environmental Science & Technology*, 33, 3755–3760, <https://doi.org/10.1021/es9904033>, <https://pubs.acs.org/doi/10.1021/es9904033>, 1999.
- Chanton, J. P., Rutkowski, C. M., Schwartz, C. C., Ward, D. E., and Boring, L.: Factors influencing the stable carbon isotopic signature of methane from combustion and biomass burning, *Journal of Geophysical Research: Atmospheres*, 105, 1867–1877, <https://doi.org/10.1029/1999JD900909>, <http://agupubs.onlinelibrary.wiley.com/doi/abs/10.1029/1999JD900909>, 2000.
- Folberth, G. A., Hauglustaine, D. A., Lathière, J., and Brocheton, F.: Interactive chemistry in the Laboratoire de Météorologie Dynamique general circulation model: model description and impact analysis of biogenic hydrocarbons on tropospheric chemistry, *Atmospheric Chemistry and Physics*, 6, 2273–2319, <https://doi.org/10.5194/acp-6-2273-2006>, <http://www.atmos-chem-phys.net/6/2273/2006/>, 2006.
- 30 Hauglustaine, D. A., Hourdin, F., Jourdain, L., Filiberti, M.-A., Walters, S., Lamarque, J.-F., and Holland, E. A.: Interactive chemistry in the Laboratoire de Météorologie Dynamique general circulation model: Description and background tropospheric chemistry evaluation, *Journal of Geophysical Research: Atmospheres*, 109, <https://doi.org/10.1029/2003JD003957>, <https://agupubs.onlinelibrary.wiley.com/doi/full/10.1029/2003JD003957>, 2004.
- Holmes, M. E., Sansone, F. J., Rust, T. M., and Popp, B. N.: Methane production, consumption, and air-sea exchange in the open ocean: An Evaluation based on carbon isotopic ratios, *Global Biogeochemical Cycles*, 14, 1–10, <https://doi.org/10.1029/1999GB001209>, <http://agupubs.onlinelibrary.wiley.com/doi/abs/10.1029/1999GB001209>, 2000.

- King, S. L., Quay, P. D., and Lansdown, J. M.: The $^{13}\text{C}/\text{12C}$ kinetic isotope effect for soil oxidation of methane at ambient atmospheric concentrations, *Journal of Geophysical Research: Atmospheres*, 94, 18 273–18 277, <https://doi.org/10.1029/JD094iD15p18273>, <http://agupubs.onlinelibrary.wiley.com/doi/abs/10.1029/JD094iD15p18273>, 1989.
- Levin, I., Bergamaschi, P., Dörr, H., and Trapp, D.: Stable isotopic signature of methane from major sources in Germany, *Chemosphere*, 26, 161–177, [https://doi.org/10.1016/0045-6535\(93\)90419-6](https://doi.org/10.1016/0045-6535(93)90419-6), <http://www.sciencedirect.com/science/article/pii/0045653593904196>, 1993.
- Reeburgh, W. S., Hirsch, A. I., Sansone, F. J., Popp, B. N., and Rust, T. M.: Carbon kinetic isotope effect accompanying microbial oxidation of methane in boreal forest soils, *Geochimica et Cosmochimica Acta*, 61, 4761–4767, [https://doi.org/10.1016/S0016-7037\(97\)00277-9](https://doi.org/10.1016/S0016-7037(97)00277-9), <http://www.sciencedirect.com/science/article/pii/S0016703797002779>, 1997.
- Rice, A. L., Butenhoff, C. L., Team, D. G., Röger, F. H., Khalil, M. A. K., and Rasmussen, R. A.: Atmospheric methane isotopic record favors fossil sources flat in 1980s and 1990s with recent increase, *Proceedings of the National Academy of Sciences*, 113, 10 791–10 796, <https://doi.org/10.1073/pnas.1522923113>, <https://www.pnas.org/content/113/39/10791>, 2016.
- Ridgwell, A. J., Marshall, S. J., and Gregson, K.: Consumption of atmospheric methane by soils: A process-based model, *Global Biogeochemical Cycles*, 13, 59–70, <https://doi.org/10.1029/1998GB900004>, <http://doi.wiley.com/10.1029/1998GB900004>, 1999.
- Sansone, F. J., Popp, B. N., Gasc, A., Graham, A. W., and Rust, T. M.: Highly elevated methane in the eastern tropical North Pacific and associated isotopically enriched fluxes to the atmosphere, *Geophysical Research Letters*, 28, 4567–4570, <https://doi.org/10.1029/2001GL013460>, <http://agupubs.onlinelibrary.wiley.com/doi/abs/10.1029/2001GL013460>, 2001.
- Saueressig, G., Bergamaschi, P., Crowley, J. N., Fischer, H., and Harris, G. W.: Carbon kinetic isotope effect in the reaction of CH_4 with Cl atoms, *Geophysical Research Letters*, 22, 1225–1228, <https://doi.org/10.1029/95GL00881>, <http://agupubs.onlinelibrary.wiley.com/doi/abs/10.1029/95GL00881>, 1995.
- Saueressig, G., Crowley, J. N., Bergamaschi, P., Brühl, C., Brenninkmeijer, C. A. M., and Fischer, H.: Carbon 13 and D kinetic isotope effects in the reactions of CH_4 with O(1 D) and OH: New laboratory measurements and their implications for the isotopic composition of stratospheric methane, *Journal of Geophysical Research: Atmospheres*, 106, 23 127–23 138, <https://doi.org/10.1029/2000JD000120>, <https://agupubs.onlinelibrary.wiley.com/doi/abs/10.1029/2000JD000120>, 2001.
- Snover, A. K. and Quay, P. D.: Hydrogen and carbon kinetic isotope effects during soil uptake of atmospheric methane, *Global Biogeochemical Cycles*, 14, 25–39, <https://doi.org/10.1029/1999GB900089>, <https://agupubs.onlinelibrary.wiley.com/doi/abs/10.1029/1999GB900089>, 2000.
- Townsend-Small, A., Tyler, S. C., Pataki, D. E., Xu, X., and Christensen, L. E.: Isotopic measurements of atmospheric methane in Los Angeles, California, USA: Influence of “fugitive” fossil fuel emissions, *Journal of Geophysical Research: Atmospheres*, 117, <https://doi.org/10.1029/2011JD016826>, <https://agupubs.onlinelibrary.wiley.com/doi/abs/10.1029/2011JD016826>, 2012.
- Tyler, S. C., Crill, P. M., and Brailsford, G. W.: $^{13}\text{C}/\text{12C}$ Fractionation of methane during oxidation in a temperate forested soil, *Geochimica et Cosmochimica Acta*, 58, 1625–1633, [https://doi.org/10.1016/0016-7037\(94\)90564-9](https://doi.org/10.1016/0016-7037(94)90564-9), <http://www.sciencedirect.com/science/article/pii/001670379405649>, 1994.
- Wang, X., Jacob, D. J., Eastham, S. D., Sulprizio, M. P., Zhu, L., Chen, Q., Alexander, B., Sherwen, T., Evans, M. J., Lee, B. H., Haskins, J. D., Lopez-Hilfiker, F. D., Thornton, J. A., Huey, G. L., and Liao, H.: The role of chlorine in global tropospheric chemistry, *Atmospheric Chemistry and Physics*, 19, 3981–4003, <https://doi.org/10.5194/acp-19-3981-2019>, <https://www.atmos-chem-phys.net/19/3981/2019/>, 2019.
- Yamada, K., Ozaki, Y., Nakagawa, F., Sudo, S., Tsuruta, H., and Yoshida, N.: Hydrogen and carbon isotopic measurements of methane from agricultural combustion: Implications for isotopic signatures of global biomass burning sources, *Journal of Geophysical Research*, 111, D16 306, <https://doi.org/10.1029/2005JD006750>, <http://doi.wiley.com/10.1029/2005JD006750>, 2006.